 DOI 10.1002/mnfr.201000086 *Mol. Nutr. Food Res.* 2010, *54*, S184–S195

RESEARCH ARTICLE

Flavone induces changes in intermediary metabolism that prevent microadenoma formation in colonic tissue of carcinogen-treated mice

Isabel Winkelmann[1], *Daniela Diehl*[2], *Doris Oesterle*[3], *Hannelore Daniel*[1] *and Uwe Wenzel*[2]

[1] Molecular Nutrition Unit, Department of Food and Nutrition, Technical University of Munich, Freising, Germany
[2] Molecular Nutrition Research, Interdisciplinary Research Center, Justus-Liebig-University of Giessen, Giessen, Germany
[3] Institute of Toxicology, Helmholtz Center Munich, German Research Center for Environmental Health, Neuherberg, Germany

Received: February 15, 2010
Revised: March 22, 2010
Accepted: March 25, 2010

Scope: Colorectal cancer is a major cause of cancer deaths worldwide with the need for improved therapeutics and adjuvants.
Methods and results: We here tested whether the secondary plant compound flavone affects the development of aberrant crypt foci and microadenomas triggered in C57BL/6J mice by 1,2-dimethylhydrazine. Ten weeks after the last 1,2-dimethylhydrazine injection, flavone was applied at 400 mg/kg body weight over 4 wk by gavage. Flavone was found to increase apoptosis and to reduce the rate of proliferation and aberrant crypt formation. More importantly, development of microadenomas was completely suppressed by flavone. Proteome analysis by 2-DE with mass spectrometric identification of regulated proteins suggests a downregulation of tricarboxylic acid cycle activity in colonocytes with compensation by increased $FADH_2$ production *via* a partial β-oxidation of long-chain fatty acids to meet energy demands. Transcriptome analysis, using a Gene Chip expression array with 24 000 gene probes confirmed the proteome data and moreover revealed the increased expression of various solute transporters, suggesting increased substrate supply to be used for tricarboxylic acid cycle-independent energy production.
Conclusion: In conclusion, changes in the levels of proteins from intermediary metabolism or their encoding mRNAs are linked to flavone-induced apoptosis and the prevention of microadenoma formation in transformed colonocytes of mice.

Keywords:
2D-PAGE / Adenomas / Flavone / Gene chips / Intermediary metabolism

1 Introduction

Colorectal cancer is the second leading cause of cancer-related deaths for both men and women in Western countries [1]. Flavonoids are secondary plant compounds considered to act as anti-tumor agents in a diet rich in fruits and vegetables [2, 3]. Selected flavonoids were shown to target molecular pathways, which can terminate tumor cell proliferation, induce apoptosis or inhibit the spread of tumor cells [4–6]. Apoptotic cell death has emerged as a prime target for treatment at various stages of tumor progression [7] and a failure to execute the apoptotic program promotes cancer development [8, 9]. We previously observed that the flavonoid flavone is a potent apoptosis inducer in HT-29 human colon cancer cells *in vitro* [10] whereas human colonocytes with a lower grade of trans-

Correspondence: Professor Uwe Wenzel, Molecular Nutrition Research, Interdisciplinary Research Center, Justus-Liebig-University of Giessen, Heinrich-Buff-Ring 26-32, D-35392 Giessen, Germany
E-mail: uwe.wenzel@ernaehrung.uni-giessen.de
Fax: +49-641-99-39229

Abbreviations: ACF, aberrant crypt foci; **DMH,** 1,2-dimethylhydrazine; **ROS,** reactive oxygen species

formation remained unaffected by this compound [11]. Moreover, *in vivo* studies in mice [12] demonstrated a significant reduction of preneoplastic lesions when flavone was subsequently or simultaneously applied with the carcinogen 1,2-dimethylhydrazine (DMH). Mechanistically, the efficient and selective eradication of transformed colonocytes by flavone appears to be due to an increase in reactive oxygen species (ROS) production as a consequence of an enhanced uptake of oxidizable substrates, such as lactate or pyruvate into mitochondria followed by increased rates of respiration [13, 14]. Whereas most cancer cells – even in the presence of sufficient oxygen – produce energy mainly from glycolysis with increased lactic acid production [15], flavone seems to force the tumor cells to use metabolic pathways characteristic for normal cells with oxidative metabolism. The characteristic aerobic glycolysis found in most tumor cells, the so-called Warburg effect, seems to limit ROS production and thereby prevents damage of DNA and proteins for the sake of a low energy yield when substrates are not completely oxidized [16]. In colonic tissue of DMH-treated mice in which preneoplastic lesions but not tumors occurred, we observed that flavone caused an increase in the expression of tricarboxylic acid cycle (TCA) enzymes. In tumor cells in culture, however, the early production of mitochondrial ROS subsequent to flavone exposure [17] was followed by a downregulation in the expression of TCA enzymes suggesting a compensatory mechanism to escape ROS-driven apoptosis [18].

In this study, we assessed whether flavone is able to interfere in later stages of tumor development beyond serving as a tumor suppressing or blocking agent *in vivo*. Tumor formation was initiated in C57BL/6J mice with the colon carcinogen DMH as described [19]. After 10 wk, an intervention trial with 400 mg flavone/kg body weight *per* day over 4 wk was performed. As the ingestion of total flavonoids in humans is suggested to lie in the range of 400 mg/day [20], the amount applied to the mice clearly reflects a pharmacological dose of the food ingredient. Appearance of aberrant crypt foci (ACF) and microadenomas served as parameters for preneoplastic and neoplastic lesions, respectively. Immunohistological staining of tissue sections for BrdU and cleaved caspase-3 was used as indicators of the anti-proliferative and anti-apoptotic activities of flavone. Transcriptome and proteome analyses were performed from tissue samples to identify the molecular mechanisms of flavone action in the intestinal tract of mice.

2 Materials and methods

2.1 Materials

Tap water and diet (V1534) for animal experiments were from Ssniff (Soest, Germany). Entellan was purchased from Merck (Darmstadt, Germany). Rabbit polyclonal cleaved caspase-3 (Asp175) antibody was from Cell Signaling (Frankfurt, Germany), biotinylated anti-rabbit IgG and the Avidin Biotin Complex Vectastain *Elite* Peroxidase-based system from Vector Laboratories (Wertheim, Germany). Antibodies for BrdU staining were from Sigma-Aldrich (Deisenhofen, Germany). TRIzol^{TM} reagent was from Invitrogen (Karlsruhe, Germany) and RNeasy spin columns from Qiagen (Hilden, Germany). Complete mini protease inhibitor cocktail tablets were purchased from Roche (Mannheim, Germany), pharmalyte, pH 3–10, the Mini dialysis kit, and linear IPG strips, pH 3–10, from Amersham Biosciences (Freiburg, Germany) and the Bio-Rad Protein Assay from Bio-Rad (Munich, Germany). Gene Chip® 3′ Expression Arrays were from Affymetrix (Santa Clara, CA, USA) as customized for NuGO (The European Nutrigenomics Organization). All other reagents, including flavone with a purity of $\geq$99.0% as determined by HPLC, were obtained from Sigma-Aldrich (Deisenhofen, Germany).

2.2 Study design

Female C57BL/6J-mice were purchased from Harlan Winkelmann (Borchen, Germany) at 4 wk of age and were divided into two groups. Tap water and diet was supplied *ad libitum* and the animals were kept on a 12-h light- and 12-h dark-cycle in a controlled temperature and humidity room with 4–5 animals *per* cage. All mice were weighed weekly and before sacrifice. For inducing ACF and microadenomas, all animals were treated with 40 mg/kg body weight DMH once a week for 5 wk by intraperitoneal injection. Effective induction of ACF in female C57BL/6J-mice was shown previously [21]. Thereafter, ACF were allowed to form for 5 wk before flavone was applied at a dose of 400 mg/kg body weight 5 days a week over 4 wk by gavage, subsequent to vigorous pulverization and suspension in 0.9% saline solution containing 0.1% of the co-surfactant Myrj 53. Control animals received the vehicle only. All animals were sacrificed 14 wk after the last injection of DMH, always between 9 and 11 am. The mice were killed by a cervical dislocation under ether anesthesia. Animal handling and experimentation were performed in accordance to the German Animal protection law and approved by the Animal Care and Use Committee of Bavaria (AZ 211-2531-37/00).

2.3 Determination of the number of ACF

ACF were counted in flat preparations of the colon in 17 animals from each group. For this purpose, the gut was removed and rinsed with ice-cold Tris buffer (pH 7.4). Thereafter, the colon was cut into parts matching the length of a slide. Before placing on slides, a stirring rod was inserted and each piece of the colon was dissected along the longitudinal axis. After placing flat on a microscopic slide with the mucosal side up, the colon was covered with a filter

paper and fixed in 10% neutral buffered formalin for 6 h. The colonic crypts were stained with 2 g/L of methylene blue in PBS for ~10–15 min. The number of ACF and the aberrant crypt multiplicity was determined by light microscopy at a magnification of 25 ×.

2.4 Immunohistochemistry

For assessing proliferative activity in colonic tissue, 2 h before sacrifice, six mice of each group were injected intraperitoneal with 30 mg/kg body weight of BrdU which is incorporated into DNA-synthesizing nuclei and can be used for the identification of S-phase cells [22]. Specimens of the colon were routinely formalin-fixed and paraffin-embedded. Serial tissue sections (3–4 μm) were prepared and mounted on glass slides. They were dewaxed, rehydrated and digested for 2 min with 0.01% trypsin before endogenous peroxidase was quenched with 3% H_2O_2 in Tris-HCl buffer pH 7.8. After blocking non-specific protein–protein interactions with 1% BSA in Tris-HCl buffer for 60 min at room temperature, the slides were incubated with a mouse-anti-BrdU monoclonal antibody, diluted 1:10 in blocking buffer, for 90 min at room temperature. Subsequently, a secondary peroxidase-conjugated antibody directed to IgG from mouse was diluted 1:10 in Tris-HCl buffer containing 1% BSA and applied to the slides for 60 min at room temperature. Slides were thoroughly washed with Tris-HCl buffer between the incubation steps. All sections were counterstained with hematoxylin and mounted in Entellan. Brown staining of nuclei indicated the cells in the S-phase.

For determination of apoptosis, immunohistochemistry for cleaved caspase-3 was performed in formalin-fixed and paraffin-embedded colonic samples. Sections were dewaxed in xylene, endogenous peroxidase was blocked in all sections with 0.5% H_2O_2 in methanol and epitope retrieval was performed by microwaving for 33 min in citrate buffer (pH 6.0) in a microwave pressure cooker at 750 W. The rabbit polyclonal cleaved caspase-3 (Asp175) antibody was diluted 1:200 in blocking buffer (5% goat serum in TBS, pH 7.6) and incubated overnight. Biotinylated anti-rabbit IgG (dilution 1:200) served as a secondary antibody. The Avidin Biotin Complex Vectastain Elite Peroxidase-based system with diaminobenzidine as the substrate served for visualization of cleaved caspase-3. Sections were counterstained as described for the BrdU staining. Staining of brown nuclei indicated cells that underwent apoptosis.

2.5 Calculations and statistics for animal experiments

Variance analysis between groups was performed by one-way ANOVA and significance of differences between control and treated mice were determined by a Tukey's multiple comparison test (GraphPadPrism, San Diego, CA, USA). For each variable at least three independent experiments were carried out. Data are given as the mean ± SEM.

2.6 Sample preparation for gene chip expression analysis and 2D-PAGE

Aliquots of homogenized complete colons from six mice of each group served for proteome and gene chip expression analysis. Tissue samples were immediately snap-frozen in liquid nitrogen after killing the mice and after colons had been removed, rinsed with Tris-buffer and crushed in a mortar in the presence of liquid nitrogen. Samples were stored in 0.1 g aliquots at −80°C until further use.

For total cellular RNA extraction, 0.03 g of the colon samples was homogenized within 1 mL of TRIzolTM reagent and purified according to the manufacturer's instructions, including a phase separation step by adding 0.2 mL of chloroform *per* 1 mL of TRIzol^{TM} reagent. The resulting RNA was then subjected to a second cleanup using RNeasy spin columns as recommended in the Affymetrix manual. RNA quality was assessed by spectrophotometric absorbance measurements at 230, 260 and 280 nm and by 1% agarose gel electrophoresis in the presence of ethidium bromide. The absorbances of the samples have to show a ratio of $A260/A280$ between 1.8 and 2.2 and $A260/A230 > 1.8$. Samples, which did not meet these criteria or which revealed approximately equal 18S and 28S ribosomal bands, indicating RNA degradation, were excluded from further study. Further preparation was performed using the provided kits and reagents. Five micrograms of total RNA was used to generate double-stranded cDNA by reverse transcription, followed by a cleanup and synthesis of biotin-labeled cRNA. After cleanup and quantification of the biotinylated cRNA, it was subjected to fragmentation and stored at −20°C until hybridization.

For protein extraction, 0.1 g of the colon samples were mixed with 1 mL of lysis buffer, containing urea (7 M), thiourea (2 M), DTT (65 mM), CHAPS (2%), Complete mini protease inhibitor cocktail tablets and pharmalyte, pH 3–10 (10%). The resultant cell lysate was sonicated for 6 × 10 s and centrifuged at 14 000 × *g* for 45 min to collect the supernatant. Lysates were precipitated with acetone overnight and dialyzed using the Mini Dialysis Kit at +4°C according to the manufacturer's instructions. The concentration of the solubilized proteins was determined using the Bradford method with the Bio-Rad protein assay.

2.7 Gene chip expression array hybridization and analysis

The Gene Chip® 3′ Expression Arrays (Affymetrix), customized for NuGO (The European Nutrigenomics Organization), were used in this study. The arrays contain about 24 000 gene sequence spots. The 16-h hybridization,

washing, staining and scanning of the cartridge arrays were performed according to the manufacturer's protocol (Affymetrix), by using the GeneChip® Hybridization Oven 640, the Fluidics Station 450 and the Scanner 3000 with Autoloader (Affymetrix). We applied internal standards to demonstrate the hybridization quality of each array. Microarrays, passing the quality control, were normalized and probe cell intensity data (.CEL file generation) were summarized by using the GeneChip 4.0 software, which enables sample and array registration, data management, fluidics and scanning instrument control as well as automatic and manual image gridding. Moreover, the methodology was approved in previous studies by Northern blotting and quantitative real-time RT-PCR [23, 24]. The statistical analysis and the comparative study of the array data in the generated .CEL files were done with the ChipInspector software (Genomatix Software, Munich, Germany). A false discovery range of 0.1% and minimum probe coverage of 4 out of 11 were chosen to get the list with identifiers of gene products and their associated regulation factors. Gene products matching these criteria were defined to be significantly regulated. The identifiers could be mapped to genes by using the Bibliosphere Pathway software (Genomatix) for analysis and interpretation of the array data.

The basis of the MeSH filter method is represented by the information gained through PubMed articles. In this study, the MeSH term ''disease'' was applied as a filter on the gene set, consisting of a hierarchy of terms itself. Using the software Bibliosphere for each of these terms, a statistical analysis is accomplished based on the number of observed and expected annotations for the terms. The resulting *Z*-scores describe whether a special annotation is over or underrepresented in the analyzed set of genes. *Z*-scores are calculated by means of observed minus expected annotations, which are divided by SD of observed annotations (Z = (observed–expected)/SD (observed)).

2.8 2D-PAGE

For the first dimension, a total protein amount of 500 μg was applied by cup-loading at the anodic end of an 18-cm-long IPG strip with immobilized broad range pH gradients, which were rehydrated overnight in solubilization buffer containing 8 M urea, 2% CHAPS, 2% pharmalyte and 13 mM DTT. Proteins were focused using the Ettan IPG Phor II from Amersham as described [25] with minor modifications. Focusing was achieved at the following conditions: 1 min at 500 V (gradient), 90 min up to 4000 V (gradient) and for a total of 25 000 V h at 8000 V (step-*n*-hold). The gel strips with the focused proteins were either frozen at −80°C or directly processed for second dimension. After equilibration with a buffer containing 6 M urea, 30% glycerol, 0.4% SDS, 50 mM Tris-buffer (pH 8.8) and either DTT or iodacetamide, the IPG strips were transferred onto a 12.5% acrylamide gel for the second dimension. One-millimeter--thick 12.5% SDS-polyacrylamide gels were cast according to the method of Laemmli [26] and were run using an Amersham Biosciences Ettan-Dalt II System employing the following conditions: 4 mA *per* gel for 1 h, then 12 mA *per* gel.

The proteins in the gels were fixed in 40% v/v ethanol and 10% v/v acetic acid for 5 h. Gels were then stained overnight in Coomassie-solution containing 10% w/v $(NH_4)_2SO_4$, 2% v/v phosphoric acid, 25% v/v methanol and 0.625% w/v CBB G250. Gels were destained in double distilled water until the background was completely clear.

2.9 Analysis of proteins using the ProteomWeaver software

Gels stained with Coomassie were scanned using an Umax scanner Power Look III (software: Magic Scan version V4.5, UMAX) and spots detected by the ProteomWeaver software (Definiens, Munich, Germany). Background subtraction and volume normalization were made automatically by the software. After spot detection, all gels were matched to each other. Six gels derived from individual mice were grouped and compared with the gels derived from six control mice, whereas a chosen protein spot had to be present in at least three of the six gels within a group. Spots differing significantly ($p < 0.05$, Mann–Whitney test) in their intensities were picked for MALDI-TOF-MS analysis.

2.10 Enzymatic digestion of protein spots and MALDI-TOF-MS

Selected Coomassie-stained spots were excised from the 2-D gels with a PROTEINEER spII spot picker (Bruker Daltonics, Leipzig). Destaining, drying and digestion were performed with the PROTEINEER dp™ workstation using the calibration and digestion kits by following the manufacturer's instructions (Bruker Daltonics). Subsequently, samples were spotted automatically by the workstation either onto an AnchorChip MALDI-target 800/384 by using α-cyano-4-hydroxy-trans-cinnamic acid as matrix, acidified by using an aqueous 0.1% TFA as washing solution and air-dried at room temperature or onto a prespotted AnchorChip target PAC384 with α-cyano-4-hydroxy-*trans*-cinnamic acid matrix for 384 samples and 96 calibration spots. Analysis was performed with an Autoflex MALDI-TOF mass spectrometer (Bruker Daltonics), operating in reflector mode with a 20-kV accelerating voltage and a 130-ns delayed extraction. Mass spectra were acquired in an automatic mode using the AutoXecute module of FlexControl software version 2.4 (Bruker Daltonics). Spectra of identical protein spots from at least four independent gels and from different treatment groups were processed with FlexAnalysis 2.4

(Bruker Daltonics), by using the smoothing option and calibrating both external, and internally with the autoproteolysis peptide of trypsin (m/z 2211.10). Background peaks such as keratin, Coomassie, *etc.*, were removed and a signal–to-noise threshold (S/N) of three was applied for the samples and six for the Peptide Calibration Standard (1000–4000 Da, Bruker Daltonics). Peptides were selected in the mass range of 800–3500 Da. The resulting mass list was evaluated using Bio Tools 3.0 with the search engine MASCOT (version 1.9.00, http://www.matrixscience.com) and the MSDB database. The criteria for positive identification of proteins were set as follows: $\pm$50–150 ppm peptide mass tolerance, 0 or 1 missed cleavage, carbamidomethyl modification of cysteine as global and methionine oxidation as variable modification and charged state as MH^+. A protein was seen as validated when three samples satisfactorily showed the same results with a probability based MOWSE score being significant ($p<0.05$) and theoretical molecular weight and pI showing at least similar results as in the gels from which they were picked.

3 Results

3.1 Flavone blocks the development of microadenomas in colonic tissue of DMH-treated mice

Administration of flavone to mice treated with DMH for the initiation of preneoplastic ACF and neoplastic microadenomas caused a significant reduction in the numbers of ACF consisting of less than four aberrant crypts (Fig. 1A). ACF with higher crypt multiplicity, generally recognized to have a higher malignant potential, remained unaffected by flavone treatment (Fig. 1A). Microadenomas, as characterized by lesions in the pericryptal region (Fig. 1B, Inset), were virtually absent in flavone-treated mice whereas they occurred regularly in controls (Fig. 1B). The prevention of microadenoma formation by flavone was associated with a significantly reduced number of proliferating cells (Fig. 1C) and an increased number of apoptotic cells (Fig. 1D). Both, proliferating cells and apoptotic cells were exclusively detected at the crypt base (Figs. 1C and D, Insets). No adverse effects or development of ACF or microadenomas were observed when flavone was applied in the absence of DMH (data not shown).

3.2 Flavone alters steady state levels of key proteins of intermediary metabolism

Proteome analysis of colonic tissue specimens from mice initially treated with DMH followed by flavone administration or vehicle control revealed a total of 603 Coomassie-stainable proteins of which 38 protein spots displayed significant alterations in the steady state levels due to flavone exposure. Of these, 33 proteins could be identified by MALDI-TOF-MS (Fig. 2 and Table 1). Among them, a number of cytoskeleton and actin-remodeling proteins responded to flavone (Table 1, Fig. 2). As many of them are substrates of caspases their altered status might be due to the initiation of apoptosis processes.

Eighteen of the regulated proteins could be allocated to have a function in intermediary metabolism (Table 1, Fig. 2). This may be taken as a measure of major alterations in metabolic pathways that could underlie the apoptosis-inducing effects of flavone. The increased β-enolase and lactate dehydrogenase levels (Table 1, Fig. 2) may account for an increased production of pyruvate or lactate in the cytosol from glucose. The levels of isocitrate dehydrogenase, identified in two protein spots with slightly different molecular weights were found significantly reduced (Table 1, Fig. 2). This may suggest that despite an increased supply of glycolytic end products the capacity of TCA *per se* is not increased. However, an increased supply of reduction equivalents in form of $FADH_2$ to the respiratory chain may be coming from increased levels of very long-chain specific acyl-CoA dehydrogenase in mitochondria (Table 1, Fig. 2). Within the acyl-CoA dehydrogenase reaction, the FAD of an electron transfer protein is reduced to subsequently transfer the electrons onto ubiquinone of complex III. The increased expression of an electron transfer protein subunit caused by flavone (Table 1, Fig. 2) stresses the importance of these adaptations to allow the metabolic shifts caused by flavone. However, fatty acid oxidation in general does not seem to be increased as the second enzyme in mitochondrial β-oxidation, enoyl-CoA hydratase, was found with reduced levels after flavone treatment (Table 1, Fig. 2).

3.3 Flavone changes transcript levels of more than one thousand genes of metabolism in colonic tissues of DMH-treated mice

The spotted gene sequences on the arrays served to detect the expression of approximately 24 000 different mouse mRNA species. Of those 3069 were found to be significantly affected in level by flavone treatment (Supporting Information 1). Employing the Bibliosphere-software the term ''disease'' was applied as a filter on the gene set. Interestingly, highest Z-scores were identified for gene sets involved in glucose metabolism preceding those for neoplasms (Table 2). Overall, gene sets with high Z-scores were almost exclusively related to glucose metabolism and to the development of neoplasms (Table 2).

Within the Bibliosphere software different filtering processes can be applied by which the regulated transcripts can be grouped according to their biological functions. Starting with the ''biological process'' filter that encompassed the highest number of regulated transcripts, additional filter settings where applied. Based on the finding that more than 1000 transcripts with a function in ''metabolism''

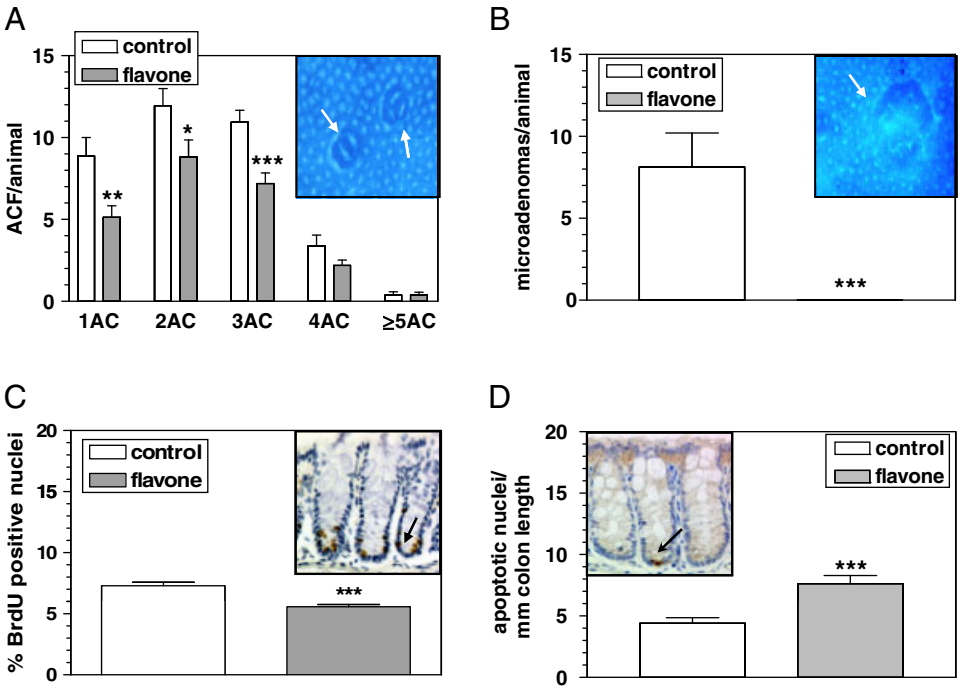

Figure 1. Flavone inhibits formation of ACF and microadenomas by reducing proliferation and causing apoptosis. Initiation of ACF and microadenomas was done by DMH-treatment. Five weeks after the last DMH-injection intervention with flavone was performed over 4 wk at a dose of 400 mg/kg body weight five times a week. Colonic tissues were stained by methylene blue for detection of ACF (A), and microadenomas (B), and by immunohistochemistry for detection of S-phase cells (C), and cleaved caspase-3 (D) as described under Materials and methods. Insets in figures show representative pictures of the parameters measured (arrows) and represent stained sections from colon transversum. $^{*}p<0.05$, $^{**}p<0.01$, $^{***}p<0.001$ *versus* the control.

were identified (Fig. 3), a second round filtering for ''glucose metabolic process'', ''fatty acid metabolic process'' and ''amino acid metabolic process'' was performed. Nineteen transcripts were identified by the ''glucose metabolic process'' filter (Supporting Information 2). Increased levels of aldolase and reduced levels of phosphoenolpyruvate carboxykinase mRNAs suggest alterations that favor glycolytic activity with a concomitant decline in the gluconeogenesis pathway. Increased levels of pyruvate dehydrogenase kinase-4 suggest that conversion of pyruvate to lactate may be increased as a result of pyruvate dehydrogenase inhibition. Thirty-three mRNAs were found to be related to fatty acid metabolism (Supporting Information 3). Although upregulated at the protein level, very long-chain specific acyl-CoA dehydrogenase was diminished by flavone at the mRNA level. Two members of long chain acyl-CoA synthetase were found upregulated whereas a medium-chain family member was downregulated. Enoyl-CoA hydratase – mitochondrial isoform – was identified as downregulated and here a reduced protein level was also observed. Reduced mRNA-levels of hydroxyacyl-coenzyme A dehydrogenase and of a trifunctional protein possessing in addition enoyl-coenzyme A hydratase and 3-ketoacyl-Coenzyme A thiolase activities were identified supporting the notion that β-oxidation of fatty acids in general may not be enhanced. Twenty-nine regulated transcripts with relevance for amino acid metabolism have been identified. In particular the down-regulation of glutamate dehydrogenase may suggest a reduced delivery of ketoacids from amino acid degradation to TCA for oxidation.

With the filter ''TCA'', six regulated transcripts coding for TCA proteins were identified with reduced levels under flavone treatment including succinate-CoA ligase, two subunits of succinate dehydrogenase, fumarate hydratase, and the dehydrogenases for malate and isocitrate (Supporting Information 4). In addition, nine transcripts involved in ''electron transport chain'' were found regulated and among them the coactivator 1α of peroxisomal proliferator-activated receptor gamma (PGC-1α) was found increased. PGC-1α can promote the transcription of enzymes necessary for substrate oxidation and electron transport. However, diminished transcript levels of four subcomplexes, two Fe–S clusters, and the flavoprotein of NADH-dehydrogenase do not support an increased respiratory chain activity.

Among the mRNAs coding for nutrient transporters, two facilitated glucose transporters, members 5 and 9, the sodium/glucose transporter-1, the fatty acid transporter-4 and several amino acid transporters, including three belonging to the cationic amino acid transporting y^{+}-system and for glutamate were significantly upregulated (Supporting Information 5).

Filtering of the transcript data sets for ''cell cycle'' and ''induction of apoptosis'' identified 152 cell cycle associated transcripts as affected by flavone with most of them altered in a direction that implies an inhibition of cell proliferation. For instance, cyclins A2, B2, D2, D3, G1, and T2 were all downregulated, as were cyclin-dependent kinase 9, a CDC2-related kinase, and cyclin-dependent kinases 2 and 7 (Supporting Information 6). Transcripts for inhibitors of cyclin-dependent kinases 1A and 2B were inversely found

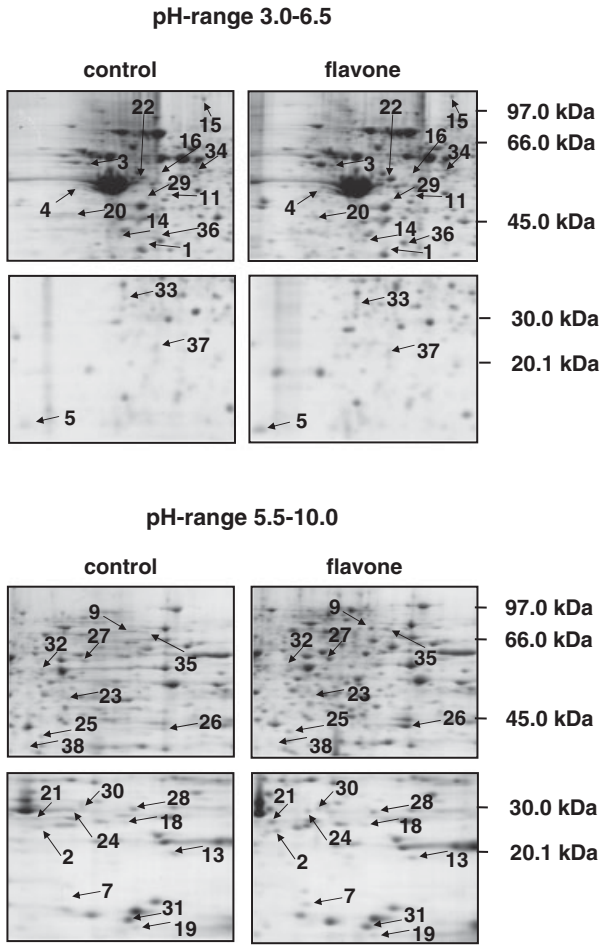

Figure 2. 2D-PAGE of proteins from colonic tissue extracts of mice treated with 400 mg flavone/kg body weight or with vehicle alone (control) 10 wk after the last DMH-application. Proteins were separated on a linear pH 3–10 IPG-strip in the first dimension and on a 12.5% SDS-polyacrylamide gel in the second dimension. Enlargements from identical sections of gels derived from separations of colon proteins from control mice or mice treated with flavone are shown.

with increased levels (Supporting Information 6). The growth arrest and DNA-damage-inducible 45 α (Gadd45α), which is able to inhibit cell cycle progression but also plays an important role in p53-induced apoptosis, was increased at the mRNA level (Supporting Information 6). Other apoptosis relevant transcripts from a total of 47 in this group were those coding for Bcl-2 interacting or related killer proteins, or death-associated proteins with increased transcript levels (Supporting Information 7). Most of the caspases, including caspase-3, showed reduced mRNA levels, whereas only caspase-8 displayed an increased mRNA level (Supporting Information 7). Since an increased apoptosis rate was found in the tissues, changes in the transcript levels of the identified genes may just serve as indicators for compensatory mechanisms as all of the encoded proteins are known to be activated by proteolytic cleavage.

4 Discussion

Commonly used strategies to treat colonic tumors target cell proliferation processes, *e.g.* by use of inhibitors of DNA topoisomerase I, an enzyme capable of removing DNA supercoils [27]. Inhibition of cell division, however, affects cell renewal of normal tissues including blood or epithelial cells in the gastrointestinal tract with the known severe side effects. More effective and specific drug interventions may arise from targeting specific attributes of cancer cells with less pronounced effects on normal cells. As early as 1924, the Nobel laureate Otto Warburg demonstrated that tumor cells exhibit an altered energy metabolism as they are metabolizing up to 20 times more glucose than normal cells [28]. However, cancer cells do not use glucose for respiration but show enhanced glycolysis rates with large quantities of lactate produced from pyruvate in the cytosol. Since these processes even proceed in the presence of high oxygen tension, this distinct metabolic phenotype is called aerobic glycolysis or the Warburg effect [29]. One might speculate that one reason for this obvious waste of energy in cancer cells with a lack of proper respiratory chain activity prevents mitochondrial ROS production that in turn protects mitochondrial and nuclear DNA from damage with detrimental effects on cell function and a loss of growth advantage [16, 30].

We have shown previously that HT-29 human colorectal cancer cells can be forced into apoptosis when cells are exposed to the flavonoid flavone [13]. Increased apoptosis was associated with enhanced mitochondrial ROS-production and an increased influx of glycolytic end-products into mitochondria followed by oxidation. Flavone could similarly induce apoptosis in HT-29 cells when instead of glucose a mixture of palmitoylcarnitine and free carnitine was supplied to cells whereas in the absence of flavone no apoptosis was observed. Additional data obtained in HT-29 cells showed that the cells have reduced carnitine levels and a reduced capacity for mitochondrial fatty acid import most likely caused by an inhibition of acylcarnitine/carnitine antiport [31]. Flavone increased mitochondrial carnitine levels and stimulated the uptake of long-chain fatty acids followed by increased β-oxidation, ROS-production and induction of apoptosis [32]. These metabolic changes in HT-29 cells caused by flavone were associated with changes in protein expression levels of various enzymes of intermediary metabolism. However, we also observed an adaptation phenomenon. When apoptosis has been initiated over 24 h by flavone, reduced levels of TCA enzymes such as succinate dehydrogenase or isocitrate dehydrogenase were observed [13, 18].

To assess whether flavone possesses a similar signature of effects in colonic tissue *in vivo*, precancerous lesions were induced in mice by the carcinogen DMH followed by flavone or vehicle (control) treatment. Tissue samples were submitted to transcriptome and proteome profiling with subsequent bioinformatic analysis for identifying the

Table 1. Proteins regulated in steady-state level by flavone in murine colon tissue samples when administered subsequently to the initiation with DMH

Protein description	Spot no.	Swiss-Prot acc. no.	Sequ. cov. (%)	Mowse Score	Peptides matched	M_w/p*I* theor.	M_w/p*I* exp.	Reg.-factor (flavone/ control)	*p*-Value
Annexins									
Annexin A4	1	P97429	25	63	5	36/5.4	34/5.4	0.45	0.03
Apoptosis									
Proteasome subunit α type-2	2	P49722	51	100	7	26/8.4	27/7.3	0.48	0.01
Chaperones									
Protein disulfide-isomerase A6 (Precursor)	3	Q922R8	37	106	10	49/5.1	54/4.8	0.49	0.04
Cytoskeleton and actin-remodeling proteins									
Actin, cytoplasmic 1	14	P60710	33	70	6	39/5.8	34/5.3	0.46	0.001
Cofilin-2	7	P45591	48	70	6	19/7.7	20/7.7	2.55	0.05
Keratin, type II cytoskeletal 8	4	P11679	23	85	9	55/5.7	51/4.7	0.49	0.04
Myosin light polypeptide 6	5	Q60605	35	70	5	17/5.6	17/3.4	2.12	0.001
Tagln2 protein, Transgelin 2	13	Q91VU2	47	110	8	26/8.4	24/8.9	0.48	0.02
Twinfilin-2	23	Q8BN77	44	88	9	40/6.2	42/6.1	1.81	0.03
Vinculin	15	Q64727	27	240	20	117/5.8	104/5.5	0.49	0.001
Detoxification enzymes									
Peroxiredoxin-5, mitochondrial (Precursor)	19	P99029	32	127	7	17/7.9	18/8.4	0.41	0.02
Gene regulating proteins									
Eef1d protein	20	Q91VK2	43	114	9	31/4.9	39/4.5	0.44	0.001
Metabolic enzymes									
Adenylate kinase isoenzyme 2, mitochondrial	24	Q9WTP6	35	90	6	26/7.2	30/7.7	0.49	0.001
α-Enolase	32	P17182	35	85	10	47/6.4	50/5.8	0.47	0.01
Aminoacylase-1	16	Q99JW2	37	93	8	46/5.9	46/6.0	0.61	0.01
ATP sulfurylase/APS kinase isoform SK2	9	Q9QYS0	24	91	7	71/7.3	65/7.7	2.18	0.01
β-Enolase	27	P21550	54	209	15	54/7.3	47/6.8	2.06	0.03
β-Lactamase-like protein 2	38	Q99KR3	44	112	8	33/5.9	34/5.6	0.49	0.02
Creatine kinase B-type	22	Q04447	35	122	9	43/5.4	46/5.6	2.15	0.02
Dihydropteridine reductase	30	Q8BVI4	45	86	5	26/7.7	30/7.8	0.46	0.001
Electron transfer flavoprotein subunit β	18	Q9DCW4	63	206	13	31/9.0	28/8.2	2.01	0.03
Enoyl-CoA hydratase, mitochondrial (Precursor)	28	Q8BH95	32	101	8	32/8.8	29/8.4	0.49	0.001
Ester hydrolase C11orf54 homolog	36	Q91V76	59	246	13	41/6.4	35/5.9	1.88	0.01
Ferritin heavy chain	37	P09528	44	86	6	19/5.4	21/5.5	0.28	0.03
Isocitrate dehydrogenase [NAD] subunit α, mitochondrial (Precursor)	29	Q9D6R2	31	102	14	40/6.3	42/5.6	0.49	0.01
Isocitrate dehydrogenase [NAD] subunit α, mitochondrial (Precursor)	11	Q9D6R2	40	102	10	40/6.2	45/5.6	0.49	0.05
L-Lactate dehydrogenase A chain	26	P06151	38	136	10	37/7.8	38/7.9	2.40	0.001
Peptidyl-prolyl cis-trans isomerase A	31	P17742	66	153	10	18/7.9	18/8.4	0.44	0.001

Table 1. Continued

Protein description	Spot no.	Swiss-Prot acc. no.	Sequ. cov. (%)	Mowse Score	Peptides matched	M_w/p*I* theor.	M_w/p*I* exp.	Reg.-factor (flavone/ control)	*p*-Value
Phosphatidylinositol transfer protein α isoform	25	P53810	43	122	7	32/6.0	36/6.5	3.12	0.02
Ribosyldihydronicotinamide dehydrogenase (quinone)	21	Q9JI75	46	83	6	26/6.6	29/7.0	0.38	0.01
Very long-chain specific acyl-CoA dehydrogenase, mitochondrial (Precursor)	35	P50544	18	110	7	71/8.9	66/8.2	2.50	0.05
Others									
Serum albumin (Fragment)	33	Q8CG74	49	81	5	24/5.5	27/4.8	0.49	0.03
Rab GDP dissociation inhibitor β	34	Q61598	39	91	11	51/5.9	51/6.0	2.37	0.02

Protein descriptions are concerning the Swiss-Prot website (http:// www.expasy.org/sprot/) with their associated primary accession numbers. Spot numbers are identical to those given in Fig. 2. Proteins altered significantly by treatment of mice with flavone at 400 mg/kg body weight as derived from analysis with the ProteomWeaver software were identified by MALDI-TOF-MS; MOWSE score, probability-based MOWSE score from MASCOT with $p<0.05$; Sequ. Cov (%), sequence coverage through the identified peptides; matched peptides, non redundant peptides taken for the identification; measured *M*/p*I*, mass values calculated by the Proteome Weaver software referring to the low-molecular-weight standard and calculated p*I* values; theoretical *M*/p*I*, mass and p*I* values taken from the MSDB database; Reg-factor (flavone/control), regulation of the intensities of the flavone-treated group compared with the control group taken from the Proteome Weaver software with $p<0.05$ (Student's *t*-test).

Table 2. *Z*-scores ($\geq$25) for gene groups regulated by flavone when the MeSH filter ''disease'' was applied

Term	*Z*-score
Glucose metabolism disorders	61
Diabetes mellitus	50
Neoplasms	49
Diabetes mellitus	48
Hypoglycemia	38
Neoplasms by site	38
Metabolic diseases	38
Digestive system neoplasms	34
Nutritional and metabolic diseases	34
Diabetes mellitus, type 2	34
Pancreatic neoplasms	33
Adenoma, Islet cell	33
Cell transformation, neoplastic	32
Endocrine system diseases	32
Neoplasms by histologic type	30
Colorectal neoplasms, hereditary non-polyposis	30
Hyperinsulinism	28
Insulinoma	26
Hyperglycemia	25

molecular targets of flavone. In analogy to the tumor cells in culture, we identified numerous genes and proteins undergoing changes in steady state levels that may indicate similar adaptive changes to flavone treatment in mice *in vivo*. Transcripts of 6 TCA enzymes including isocitrate and succinate dehydrogenase and fumarate hydratase were found with reduced levels and isocitrate dehydrogenase was also found reduced in protein level (Fig. 4). These changes observed *in vivo* were associated with reduced cell proliferation and increased apoptosis rates in the colonic tissues and thereby mimic similar observations made in HT-29 cells. A downregulation of succinate dehydrogenase and fumarate hydratase levels (Fig. 4) may be interpreted as a direct survival strategy since both proteins have been identified as classic tumor suppressors and mutations in both have been linked to the stabilization of hypoxia-inducible factor-1 which affects gene expression, metabolism, cell survival, tumorigenesis and tumor growth [33–35]. The mechanism by which the regulation of this factor is achieved seems *via* its prolyl-hydroxylation which promotes proteasomal degradation. The prolyl-hydroxylation requires α-ketoglutarate as a substrate. A deficiency of succinate dehydrogenase or fumarate hydratase could decrease α-ketoglutarate levels [32] and a reduced level of glutamate dehydrogenase (Fig. 4) as found here as well would in addition reduce α-ketoglutarate availability from amino acids. The latter might block as well the usage of glutamine as an oxidative substrate from the blood plasma in colonic differentiated epithelial cells [36]. The observed down-regulation of TCA enzymes and the reduced protein levels of the flavoprotein of NADH-dehydrogenase found *in vitro* as well as here *in vivo* (Fig. 4) would deprive cells of

reduction equivalents for the respiratory chain. However, we also observed increased protein levels of long-chain fatty acid dehydrogenases in the colonic tissues of flavone-treated mice (Fig. 4) similar to an upregulation found in HT-29 cells [18]. It must be stressed here that long-chain acyl-CoA dehydrogenase was decreased at its transcript level, showing that certain proteins are mainly regulated by controlling their stability or degradation and not *via* alterations of transcription or mRNA stability. Although the increased protein levels of acyl-CoA dehydrogenase may indicate an increased capacity for fatty acid oxidation, the next necessary protein in the β-oxidation cycle, the enoyl-CoA hydratase, and the final enzyme that releases acetyl-CoA, the 3-keto-thiolase, were found with lower expression levels. Yet, the initial step of fatty acid oxidation provides $FADH_2$ for transfer of electrons to complex III of the respiratory chain which may maintain a sufficient electron flow (Fig. 4). Most interestingly, complex III is the major site of ROS formation [37–40], so that ROS-production and ROS-driven apoptosis may be sustained despite an assumed reduced TCA activity. These adaptations in colonic tumor cells which may originate from the need to meet the energy demand by alternative pathways may also contribute to the differences observed regarding microadenoma formation. When mice were treated under identical conditions as in the present study but with a lower flavone dose (15 mg/kg body weight) similar proteins and similar effects were observed (unpublished). However, only with the present high dose of flavone was the electron transfer flavoprotein found upregulated (Fig. 4) and microadenoma formation prevented.

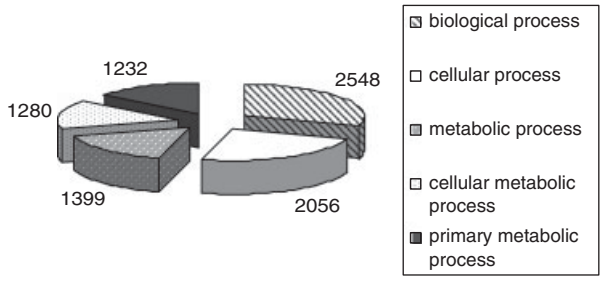

Figure 3. Allocation of regulated transcripts to distinct processes according to the Bibliosphere-software. Of the 1381 process-filters applied, the 5 that screened the highest numbers of transcripts are given in the figure.

An indication for a shift in the metabolic phenotype of mouse colon *in vivo* toward a Warburg effect is provided by increased expression of glucose transporters, lactate dehydrogenase, aldolase and enolase. The enhanced expression of pyruvate dehydrogenase kinase-4 (Fig. 4) may assist the blockade of TCA by inhibition of the pyruvate dehydrogenase complex with a concomitant reduction in the conversion of pyruvate to acetyl-CoA and increased cytosolic lactate production. Cytosolic needs of ATP may be met by this adaptive mechanisms whereas mitochondrial ATP may be derived *via* the electron transport chain driven by $FADH_2$ derived from a partial break-down of long chain fatty acids provided *via* increased fatty acid uptake into cells. This process however would still maintain a ROS-production and ROS-mediated apoptosis although the ''Warburg adaptation'' of cell metabolism is thought to prevent ROS-generation in the respiratory chain for protection of DNA damage. In this

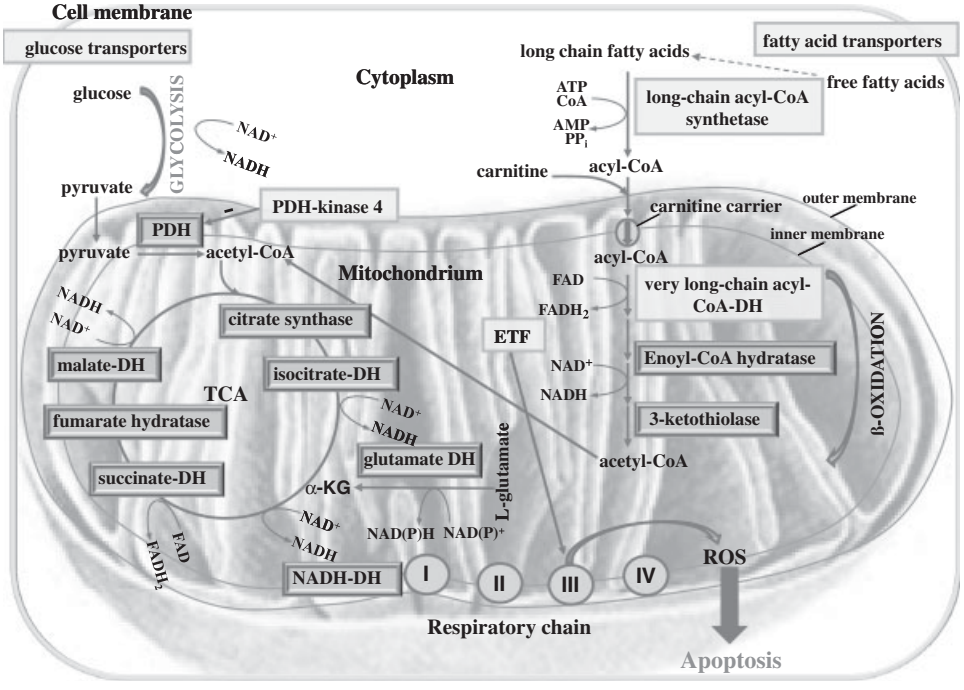

Figure 4. Model summarizing the adaptations of colonocytes to flavone *in vivo* at the mitochondrial level. Upregulated factors are presented in light-colored boxes whereas down-regulated factors are shown in dark-colored boxes. For very long-chain dehydrogenase regulation at the protein level is shown. DH, dehydrogenase; PDH, pyruvate dehydrogenase; ETF, electron transfer flavoprotein; α-KG, α-ketoglutarate.

context it has to be discussed how non-transformed colonocytes might respond to flavone. Less transformed colonocytes than those observed in the present study were shown to increase the levels of TCA proteins in response to flavone [12]. Taking into account that butyrate causes very similar regulations of genes involved in all parts of the total energy metabolism and ATP production in colonocytes of healthy human volunteers *in vivo* [41], it must be suggested that flavone and butyrate share a common mode of action for cancer prevention. It is interesting to note that normal colonocytes cope with the inevitable increase in ROS-production by butyrate with increased glutathione production [42] as well as enhanced levels of glutathione-*S*-transferase [43] and that we did find increases of glutathione-synthetase and glutathione-*S*-transferase in colonocytes with a low transformation grade in mice treated with flavone [12].

In conclusion, our studies show that flavone blocks the development of microadenomas in colonic tissue of DMH-treated mice. An increased supply of energy substrates by a pleiotropic upregulation of solute carriers in transformed tissue is suggested to provide an initially enhanced substrate flow for ATP production at the expense of increased mitochondrial ROS generation. Transcript as well as protein data strongly suggest that in response TCA activity is reduced leading to a lower supply of $NADH_2$ to the respiratory chain. This may be compensated by an increased use to fatty acids with a partial β-oxidation that yields $FADH_2$ for maintaining electron flow through the respiratory chain and also ROS production and ROS-driven apoptosis.

This study was supported by the Deutsche Forschungsgemeinschaft; Grant number: WE 2684/3-1 and 3-2. The authors greatly acknowledge the expert technical assistance of Mrs. Carmen Spiller, Mrs. Marianne Berauer and Mrs. Beate Rauscher. The authors acknowledge Mr. Alan McDonley for critically reading the manuscript. UW is a member of MITOFOOD COST Action Number FA0602.

The authors have declared no conflict of interest.

5 References

[1] Schulmann, K., Reiser, M., Schmiegel, W., Colonic cancer and polyps. *Best Pract. Res. Clin. Gastroenterol.* 2002, *16*, 91–114.

[2] Mason, J. B., Nutritional chemoprevention of colon cancer. *Semin. Gastrointest. Dis.* 2002, *13*, 143–153.

[3] Shibata, A., Paganini-Hill, A., Ross, R. K., Henderson, B. E., Intake of vegetables, fruits, beta-carotene, vitamin C and vitamin supplements and cancer incidence among the elderly: a prospective study. *Br. J. Cancer* 1992, *66*, 673–679.

[4] Plaumann, B., Fritsche, M., Rimpler, H., Brandner, G. *et al.*, Flavonoids activate wild-type p53. *Oncogene* 1996, *13*, 1605–1614.

[5] Gerritsen, M. E., Flavonoids: inhibitors of cytokine induced gene expression. *Adv. Exp. Med. Biol.* 1998, *439*, 183–190.

[6] Gosse, F., Guyot, S., Roussi, S., Lobstein, A. *et al.*, Chemopreventive properties of apple procyanidins on human colon cancer-derived metastatic SW620 cells and in a rat model of colon carcinogenesis. *Carcinogenesis* 2005, *26*, 1291–1295.

[7] Huerta, S., Goulet, E. J., Livingston, E. H., Colon cancer and apoptosis. *Am. J. Surg.* 2006, *191*, 517–526.

[8] Hanahan, D., Weinberg, R. A., The hallmarks of cancer. *Cell* 2000, *100*, 57–70.

[9] White, M. K., McCubrey, J. A., Suppression of apoptosis: role in cell growth and neoplasia. *Leukemia* 2001, *15*, 1011–1021.

[10] Wenzel, U., Kuntz, S., Brendel, M. D., Daniel, H., Dietary flavone is a potent apoptosis inducer in human colon carcinoma cells. *Cancer Res.* 2000, *60*, 3823–3831.

[11] Wenzel, U., Kuntz, S., Daniel, H., NO-levels in human preneoplastic colonocytes determine their susceptibility towards anti-neoplastic agents. *Mol. Pharmacol.* 2003, *64*, 1494–1502.

[12] Winkelmann, I., Diehl, D., Oesterle, D., Daniel, H. *et al.*, The suppression of aberrant crypt multiplicity in colonic tissue of 1,2-dimethylhydrazine-treated C57BL/6J mice by dietary flavone is associated with an increased expression of Krebs cycle enzymes. *Carcinogenesis* 2007, *28*, 1446–1454.

[13] Wenzel, U., Schoberl, K., Lohner, K., Daniel, H., Activation of mitochondrial lactate uptake by flavone induces apoptosis in human colon cancer cells. *J. Cell. Physiol.* 2005, *202*, 379–390.

[14] Wenzel, U., Nickel, A., Daniel, H., Melatonin potentiates flavone-induced apoptosis in human colon cancer cells by increasing the level of glycolytic end products. *Int. J. Cancer* 2005, *116*, 236–242.

[15] Kim, J. W., Dang, C. V., Cancer's molecular sweet tooth and the Warburg effect. *Cancer Res.* 2006, *66*, 8927–8930.

[16] Brand, K. A., Hermfisse, U., Aerobic glycolysis by proliferating cells: a protective strategy against reactive oxygen species. *FASEB J.* 1997, *11*, 388–395.

[17] Wenzel, U., Kuntz, S., Jambor de Sousa, U., Daniel, H., Nitric oxide suppresses apoptosis in human colon cancer cells by scavenging mitochondrial superoxide anions. *Int. J. Cancer* 2003, *106*, 666–675.

[18] Herzog, A., Kindermann, B., Döring, F., Daniel, H. *et al.*, Pleiotropic molecular effects of the pro-apoptotic dietary constituent flavone in human colon cancer cells identified by protein and mRNA expression profiling. *Proteomics* 2004, *4*, 2455–2464.

[19] Newell, L. E., Heddle, J. A., The potent colon carcinogen, 1,2-dimethylhydrazine induces mutations primarily in the colon. *Mutat. Res.* 2004, *564*, 1–7.

[20] Zamora-Ros, R., Andres-Lacueva, C., Lamuela-Raventós, R. M., Berenguer, T. *et al.*, Estimation of dietary sources and flavonoid intake in a Spanish adult population (EPIC-Spain). *J. Am. Diet. Assoc.* 2010, *110*, 390–398.

[21] McLellan, E. A., Bird, R. P., Aberrant crypts: potential preneoplastic lesions in the murine colon. *Cancer Res.* 1988, *48*, 6183–6186.

[22] Schipper, D. L., Wagenmans, M. J., Peters, W. H., Wagener, D. J., Significance of cell proliferation measurement in gastric cancer. *Eur. J. Cancer* 1998, *34*, 781–790.

[23] tom Dieck, H., Döring, F., Roth, H. P., Daniel, H., Changes in rat hepatic gene expression in response to zinc deficiency as assessed by DNA arrays. *J. Nutr.* 2003, *133*, 1004–1010.

[24] tom Dieck, H., Döring, F., Fuchs, D., Roth, H. P. *et al.*, Transcriptome and proteome analysis identifies the pathways that increase hepatic lipid accumulation in zinc-deficient rats. *J. Nutr.* 2005, *135*, 199–205.

[25] Görg, A., Obermaier, C., Boguth, G., Harder, A. *et al.*, The current state of two-dimensional electrophoresis with immobilized pH gradients. *Electrophoresis* 2000, *21*, 1037–1053.

[26] Laemmli, U. K., Cleavage of structural proteins during the assembly of the head of bacteriophage T4. *Nature* 1970, *227*, 680–685.

[27] Koster, D. A., Palle, K., Bot, E. S., Bjornsti, M. A. *et al.*, Antitumour drugs impede DNA uncoiling by topoisomerase I. *Nature* 2007, *12*, 213–217.

[28] Warburg, O., Posener, K., Negelein, E., Über den Stoffwechsel der Carcinomzelle. *Biochem. Z.* 1924, *152*, 309–344.

[29] Warburg, O., On the origin of cancer cells. *Science* 1956, *123*, 309–314.

[30] Powers, J. T., Hong, S., Mayhew, C. N., Rogers, P. M. *et al.*, E2F1 uses the ATM signaling pathway to induce p53 and Chk2 phosphorylation and apoptosis. *Mol. Cancer Res.* 2004, *2*, 203–214.

[31] Wenzel, U., Nickel, A., Daniel, H., Increased mitochondrial palmitoylcarnitine/carnitine countertransport by flavone causes oxidative stress and apoptosis in colon cancer cells. *Cell. Mol. Life Sci.* 2005, *62*, 3100–3105.

[32] Wenzel, U., Nickel, A., Daniel, H., Increased carnitine-dependent fatty acid uptake into mitochondria of human colon cancer cells induces apoptosis. *J. Nutr.* 2005, *135*, 1510–1514.

[33] Selak, M. A., Armour, S. M., MacKenzie, E. D., Boulahbel, H. *et al.*, Succinate links TCA cycle dysfunction to oncogenesis by inhibiting HIF-alpha prolyl hydroxylase. *Cancer Cell* 2005, *7*, 77–85.

[34] Wouters, B. G., Koritzinsky, M., Hypoxia signalling through mTOR and the unfolded protein response in cancer. *Nat. Rev. Cancer* 2008, *8*, 851–864.

[35] Pollard, P. J., Wortham, N. C., Tomlinson, I. P., The TCA cycle and tumorigenesis: the examples of fumarate hydratase and succinate dehydrogenase. *Ann. Med.* 2003, *35*, 632–639.

[36] Firmansyah, A., Penn, D., Lebenthal, E., Isolated colonocyte metabolism of glucose, glutamine, n-butyrate, and beta-hydroxybutyrate in malnutrition. *Gastroenterology* 1989, *97*, 622–629.

[37] Turrens, J. F., Superoxide production by the mitochondrial respiratory chain. *Biosci. Rep.* 1997, *17*, 3–8.

[38] Lenaz, G., Role of mitochondria in oxidative stress and ageing. *Biochim. Biophys. Acta Bioenerg.* 1998, *1366*, 53–67.

[39] Finkel, T., Holbrook, N. J., Oxidants, oxidative stress and the biology of ageing. *Nature* 2000, *408*, 239–247.

[40] Raha, S., Robinson, B. H., Mitochondria, oxygen free radicals, disease and ageing. *Trends Biochem. Sci.* 2000, *25*, 502–508.

[41] Vanhoutvin, S. A., Troost, F. J., Hamer, H. M., Lindsey, P. J. *et al.*, Butyrate-induced transcriptional changes in human colonic mucosa. *PLoS One* 2009, *4*, e6759.

[42] Hamer, H. M., Jonkers, D. M., Bast, A., Vanhoutvin, S. A. *et al.*, Butyrate modulates oxidative stress in the colonic mucosa of healthy humans. *J. Clin. Nutr.* 2009, *28*, 88–93.

[43] Ebert, M. N., Klinder, A., Peters, W. H., Schäferhenrich, A. *et al.*, Expression of glutathione S-transferases (GSTs) in human colon cells and inducibility of GSTM2 by butyrate. *Carcinogenesis* 2003, *24*, 1637–1644.

